Tellus (1990), *42A*, 615–626

A re-examination of the seiche periods of Lake Vättern

By GÖRAN G. A. BJÖRK and PETER A. LUNDBERG, *Department of Oceanography, Gothenburg University Box 4038, S-40040 Gothenburg, Sweden*

(Manuscript received 31 March 1989; in final form 9 November 1989)

ABSTRACT

A newly developed perturbation technique for resolving Chrystal's classical seiche problem has been applied to Vättern, a deep and elongated lake in central Sweden. Theoretical predictions of the standing-wave periods were compared to those obtained from spectral analysis of a 3-month water level record. The results for the gravest-mode seiche were found to be in good agreement, whereas the second- and third-mode predictions showed a systematic deviation from the observations. A sensitivity analysis of the computational procedure indicates that this discrepancy can most likely be ascribed to insufficient knowledge of the detailed topography of the lake.

1. Introduction

The study of barotropic standing waves in enclosed basins has been a recurrent theme within limnology and physical oceanography ever since Forel in the 1870s conducted the first systematic investigation of the phenomenon as observed in Lake Geneva. A well-known study of this type was undertaken by Bergsten (1926) for Vättern, an elongated and rather deep lake in central Sweden, extending 120 km in a direction from roughly north to south (cf. Fig. 1). This pioneering investigation was based on four extensive series of limnograph recordings at various positions along the lake which had been obtained by the Swedish Meteorological and Hydrological Agency (SMHA) in the years 1910 to 1925. From these measurements, Bergsten not only determined the periods associated with the 6 gravest standing-wave modes of the lake, but could also locate the approximate positions of the nodal points for the two most fundamental of these seiches. He furthermore showed that numerical predictions based on the Chrystal (1904, 1905) theory of seiches were in good agreement with these empirical results. Bergsten's results were impressive, not least in view of the computational aids which were available at the time of the inquiry, and have been extensively quoted ever since they were published. In particular, his graph demonstrating phase-shifted simultaneous lake-end recordings of a uninodal seiche has received widespread attention and is reproduced in many textbooks (e.g., Defant, 1961; LeBlond and Mysak, 1978).

It would be difficult, even against the background of present-day technical resources, to improve much in the design and execution of Bergsten's field experiment. In view, however, of the remarkable advances which have been made in statistical data processing over the last decades, the present authors decided to undertake a fresh survey of the seiching of the lake. The field study to be reported here was conducted on a much more modest scale than the original experimental investigation described above, and only involved a single water level gauge which was mounted on a pier in Jönköping harbour at the southern end of the lake. The recordings over a 3-month period were subjected to statistical analysis, and the results were found to conform quite well to those of Bergsten. The experimental data was furthermore compared with predictions based on a newly developed generalization (Lundberg, 1990) of the classical Ertel (1933) technique for determining seiche periods from Chrystal's equation.

In Section 2, recursive formulae for this

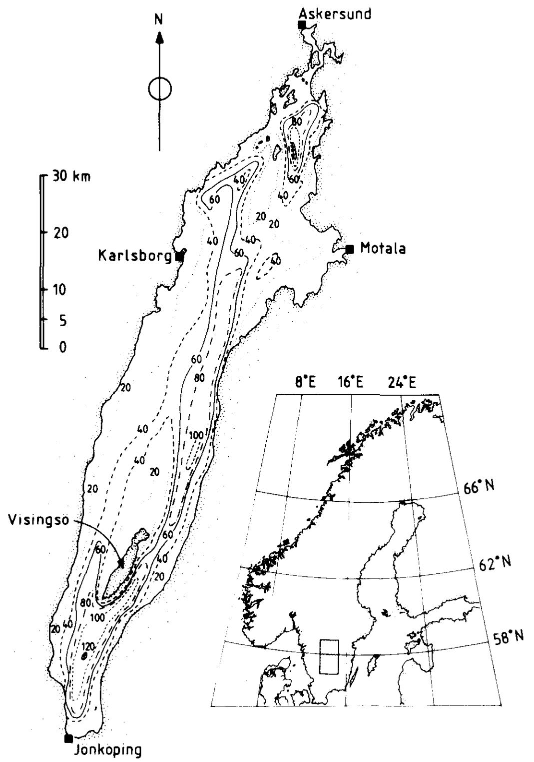

Fig. 1. Map of Lake Vättern where the water level gauge was located in Jönköping harbour. A quasi-autonomous, deep basin at the southerly end of the lake is delimited to the north by the island of Visingsö.

perturbative method are derived for an arbitrary, although elongated, lake topography. Section 3 deals with the analysis of the field data and furthermore includes a direct comparison between these results and theoretical predictions obtained by applying the computational algorithm to Bergsten's topographical data. Since the higher-mode results proved to be somewhat inconsistent with the observations, it was decided to attempt to resolve this disquieting feature of the analysis by examining the effects of alternative discretizations of the lake topography, a task which is described at some length in Section 4. A sensitivity analysis is undertaken in Section 5, and the entire study is concluded with a review of the results obtained and a discussion of the prospects for future work.

2. Theoretical considerations

We here limit ourselves to examining the seiche problem in its most simplified form, i.e., small-amplitude inviscid motion in a shallow elongated basin of moderately varying cross-section. By reformulating the longitudinal velocity as the time-derivative of the horizontal particle displacement and making use of a cross-sectionally integrated equation of continuity, the linearized horizontal equation of motion may be cast in the following form:

$$\frac{\partial^2 \varphi(v,t)}{\partial t^2} = g\sigma(v)\frac{\partial^2 \varphi(v,t)}{\partial v^2} \tag{2.1}$$

Here $\varphi(v, t)$ is the horizontal bulk displacement of the water mass, g is the acceleration due to gravity, v is a horizontal coordinate expressed in terms of the accumulated surface area, and $\sigma(v)$ is the normal curve of the lake, viz., the product of the surface width and cross-section at location v. This equation (Chrystal, 1904) governs longitudinal wave motion in the basin, and is most conveniently resolved mathematically by using the "Ansatz" $\varphi(v, t) = \psi(v)\,\zeta(t)$, $\zeta''/\zeta = -\lambda$; $\lambda > 0$. After separation of variables and imposing no-flux boundary conditions at the limiting points of the basin ($v = 0$, L), an eigenvalue problem is obtained from which the periods of the standing oscillation $T = 2\pi/\sqrt{\lambda}$ can be found:

$$\frac{d^2 \psi(v)}{dv^2} + \frac{\lambda}{g\sigma(v)}\psi(v) = 0, \tag{2.2}$$

$$\psi(0) = \psi(L) = 0. \tag{2.3}$$

Chrystal's (1905) method of solution for this problem was based on piecewise approximation of the normal curve with low-degree polynomials. Hereafter, the governing equation could be resolved analytically, ultimately yielding the eigenvalue λ as the solution to a purely algebraic problem.

In the present study, the formal eigenvalue problem will instead be analyzed using a perturbative procedure (Lundberg, 1990). A suitable expansion parameter ε is obtained by reformulating the normal curve $\sigma(v)$ in terms of its deviation from a constant value, i.e., $\sigma(v) = S(1 - \varepsilon h(x))$, where S is the maximum value of the product of basin surface width and cross-section, and $x = v/A$ is a dimensionless horizontal coordinate (where A is the total surface area of the basin). The governing equation assumes the following nondimensionalized form:

$$\frac{d^2 \psi(x)}{dx^2} + \frac{\lambda}{1 - \varepsilon h(x)} \psi(x) = 0. \tag{2.4}$$

Here the parameter $A/\sqrt{gS}$ has been incorporated in the time-scale of the problem. Due to constraints imposed by the topography of natural lakes, the final evaluation of all results will be undertaken for $\varepsilon = 1$, but for the time being this quantity is left unspecified and solely regarded as a small parameter. It is hence postulated that ψ and λ can be expanded in powers of ε:

$$\psi(x) = \sum_{m=0}^{\infty} \psi^{(m)}_{(x)} \varepsilon^m; \quad \lambda = \sum_{m=0}^{\infty} \lambda^{(m)} \varepsilon^m \tag{2.5, 6}$$

Insertion of these expressions in eq. (2.4) and ordering yields:

$$\varepsilon^0: \frac{d^2 \psi^{(0)}}{dx^2} + \lambda^{(0)} \psi^{(0)} = 0, \tag{2.7}$$

$$\varepsilon^1: \frac{d^2 \psi^{(1)}}{dx^2} + \lambda^{(0)} \psi^{(1)} = h(x) \frac{d^2 \psi^{(0)}}{dx^2} - \lambda^{(1)} \psi^{(0)}, \tag{2.8}$$

$$\varepsilon^m: \frac{d^2 \psi^{(m)}}{dx^2} + \lambda^{(0)} \psi^{(m)} = h(x) \frac{d^2 \psi^{(m-1)}}{dx^2} - \sum_{k=1}^{m-1} \lambda^{(k)} \psi^{(m-k)} - \lambda^{(m)} \psi^{(0)}, \quad m \geqslant 2. \tag{2.9}$$

These equations to all orders are associated with the homogeneous boundary conditions $\psi^{(m)}(0) = \psi^{(m)}(1) = 0$. The zeroth-order problem has the following solution:

$$\lambda^{(0)}_n = n^2 \pi^2, \quad \psi^{(0)}_n(x) = \sqrt{2} \sin n\pi x, \quad n = 1, 2, \ldots$$

It is now assumed that $\psi^{(1)}_n(x)$ can be expressed in terms of this complete set of eigenfunctions:

$$\psi^{(1)}_n(x) = \sum_{k=1}^{\infty} b^{(1)}_{nk} \sqrt{2} \sin k\pi x.$$

This expansion (which satisfies the first-order boundary conditions) and the lowest-order solution are hereafter inserted in eq. (2.8). The resulting expression, after multiplication with $\sqrt{2}$ sin πx and integration over the interval [0, 1], yields the following first-order correction formulae:

$$\lambda^{(1)}_n = -2n^2 \pi^2 \int_0^1 h(x) \sin n\pi x \sin n\pi x \, dx, \quad j = n,$$

$$b^{(1)}_{nj} = -\frac{2n^2}{n^2 - j^2} \int_0^1 h(x) \sin n\pi x \sin j\pi x \, dx, \quad j \neq n.$$

Note here that the coefficient $b^{(1)}_{nn}$ is as yet undetermined.

Proceeding to the mth order problem and expanding $\psi^{(m)}_n(x)$ in the zeroth-order eigenfunctions, a generalization of the analysis above yields the following result:

$$\lambda^{(m)}_n = -\sum_{l=1}^{\infty} b^{(m-1)}_{nl} 2l^2 \pi^2 \int_0^1 h(x) \sin l\pi x \sin n\pi x \, dx - \sum_{k=1}^{m-1} \lambda^{(k)}_n b^{(m-k)}_{nn}, \quad j = n, \tag{2.10}$$

$$b^{(m)}_{nj} = -\frac{1}{\pi^2 (n^2 - j^2)} \left(\sum_{l=1}^{\infty} b^{(m-1)}_{nl} 2l^2 \pi^2 \times \int_0^1 h(x) \sin l\pi x \sin j\pi x dx + \sum_{k=1}^{m-1} \lambda^{(k)}_n b^{(m-k)}_{nj} \right), \quad j \neq n. \tag{2.11}$$

The hitherto unspecified coefficients $b^{(m)}_{nn}$ may be determined from the normalization condition:

$$\int_0^1 [\psi(x)]^2 \, dx = 1.$$

Insertion of the power series (2.5) in this expression and ordering in ε ultimately yields:

$$b^{(1)}_{nn} = 0, \quad b^{(m)}_{nn} = -\tfrac{1}{2} \sum_{k=1}^{m-1} \sum_{j=1}^{\infty} b^{(k)}_{nj} b^{(m-k)}_{nj}, \quad m \geqslant 2.$$

From a formal standpoint, the problem is now fully resolved to arbitrary order, since a recursive procedure for determining the eigensolutions and characteristic values has been derived. As will be evident, however, a number of practical problems associated with the numerical implementation of this scheme remain to be solved.

The results above represent an extension of the classical theory due to Ertel (1933), who limited his analysis of Chrystal's equation to formulating the first-order eigenvalue correction. A technically related analysis for the somewhat more complex case of the wave-equation in non-canonical form (valid for a strictly two-dimensional basin) has been given by Lundberg (1990). Note finally, however, that the classical seiche problem

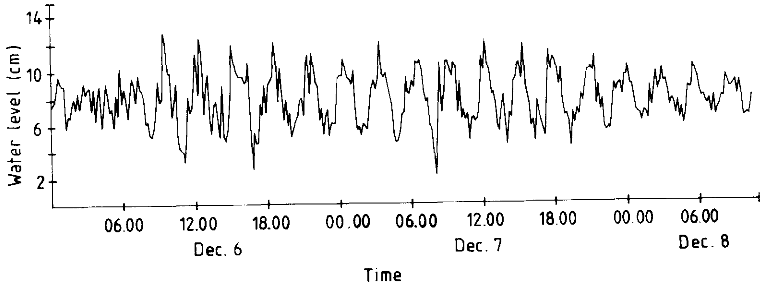

Fig. 2. Recording of the water leel at Jönköping during a 60-h period in December 1985. The gravest-mode seiche with a peak-to-peak amplitude of around 8 cm and a period of approximately 3 h is clearly visible.

dealt with in all these studies is somewhat idealized; for a review of modern developments in the field such as including the effects of the earth's rotation and the curvature of the basin axis, cf., Raggio and Hutter (1982).

3. Field investigation and comparison with theory

The water level recordings in the form of discrete measurements every 10 min were made from a pier in Jönköping harbour from 25 October 1985 until 2 February 1986, at which time the lake froze over. This period of observation was selected after a study of climatological data had suggested that the maximum amount of stormy weather occurred during autumn, hereby increasing the likelihood that the free barotropic oscillation modes might be excited in the lake. The recordings were made with a differential pressure gauge, thus eliminating the necessity to compensate for barometric variations. A linearly interpolated segment of the unprocessed time series is shown in Fig. 2, where a gravest-mode standing wave with an amplitude of around 4 cm and a period of approximately 3 h is evident. The onset of the seiching motion is quite drastic, whereafter the standing wave is slowly damped out. (The maximum amplitude of this fundamental oscillation observed during the entire experiment was 6 cm.)

In order to prepare the time-series for statistical analysis, slow changes were removed from the data set using a Butterworth filter (Båth, 1974) with a half-power point of 6 h. (During the experiment, the overall water level varied over a 40-cm range, due not only to the precipitation over the lake and its drainage basin, but also to a fluctuating runoff controlled by the hydro-electric power plant in Motala.) The spectral characteristics of the de-trended residual time series consisting of around 10^4 records were hereafter determined using standard techniques (Båth, 1974), and in Fig. 3, the resulting power spectrum is shown. Three significant peaks associated with the gravest modes of the standing oscillation are clearly in evidence with the periods $T_1 = 179.5$, $T_2 = 97.0$ and $T_3 = 80.5$ min. These results were found to be in good agreement with Bergsten's observations (and consequently also with his theoretical predictions). A noteworthy feature of the data set is that no significant information could be extracted for frequencies beyond those demonstrated in Fig. 3; hence, no indication of autonomous seiching motion in the Jönköping-Visingsö basin was discernible in the spectral results. A further discrepancy with Bergsten's study is that during the experiment reported here, no standing oscillations of mode number higher than three were observed. However, in view of the fact that the data upon which Bergsten (1926) based his period estimates had been culled in a highly selective fashion from water-level records covering around 30 gauge-years, this shortcoming of the present investigation should not be taken too seriously.

The good correspondence with Bergsten's data tended to further reinforce confidence in the experimental appraisals of the seiche periods. These observations may now be compared with the standing-wave periods predicted using the perturbative scheme derived in Section 2. Before this algorithm can be applied, however, the rather intricate question must be settled of how to

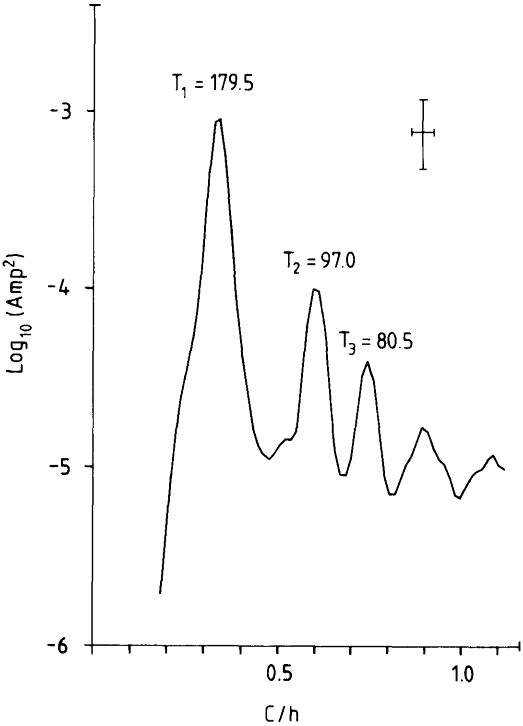

Fig. 3. Power spectrum of the water level recordings where the three distinct peaks may be associated with the gravest modes of the standing oscillation. A 95% confidence limit is also shown. The spectrum, based on consecutive sets of 2000 recordings, is smoothed by a Parzen window with a cut-off point equal to 200. It did not contain any significant information beyond the 1.1 cycle/h limit of the graph.

best accomplish a useful Fourier representation of the normal curve in Chrystal's equation. Several different possibilities have been explored on the basis of Bergsten's original 28-point discretization of $\sigma(v)$ for Lake Vättern, where $S = 21.19$ km^3 and $A = 1890.0$ km^2. Fourier decompositions to arbitrary order of either a linearly interpolated normal curve or Bergsten's piecewise polynomial approximation both proved to have the drawback that spurious effects were induced in the analysis by Gibb's phenomenon occurring at the junction points between the segments, where discontinuous first derivatives of $\sigma(v)$ were the rule. It was finally decided instead to represent Bergsten's topographical data using a straightforward 28-component Fourier-cosine expansion. A related question concerns where to terminate the infinite summations occurring in the general recursive formulae (2.10, 11). An extensive set of numerical experiments showed that a 50-term approximation in all cases provided ample margins, and hence the results to be reported here have been calculated for this limit. The convergence radii of the perturbation series have been determined using a graphical version of Cauchy's ratio test (Domb and Sykes, 1957). In Fig. 4, the results for the gravest modes of the eigenvalue expansion (2.5) are shown, and from this graph, it is recognized that for each of these three power series, the radius of convergence is significantly larger than 1, since it is the reciprocal of the extrapolated intercept at $1/n = 0$. Although not shown here, analogous results were obtained over the entire interval (0, 1) for the corresponding eigenfunction expansions (2.6). A truncation level which must finally be decided upon before any evaluation of the eigenvalues determining the seiche periods can be carried out, is to which order N in ε the perturbation series (2.5, 6) are to be calculated. The present results (cf. Table 1) partly circumvent this question by showing the outcome of the analysis for $N = 10$, 20, 50 and 100. In this context, it must furthermore be underlined that all values in the table have been obtained for $\varepsilon = 1$, in accordance with the considerations of Section 2. This value of the perturbation parameter is located well within the circle of convergence of the expansions, and hence the power series (2.5, 6) converged in an adequate fashion even for this rather large value of ε. In order to further increase their rates of convergence, however, a nonlinear transformation of the partial sums (Shanks, 1955) has also been applied when computing the results of Table 1.

The present investigation has primarily restricted itself to examining the periods of the standing oscillations, since the rather modest field experiment did not permit any far-reaching conclusions about the spatial characteristics of the seiches. The eigenfunctions $\psi_n(x)$, $n = 1, 2, 3$ associated with the gravest modes of the standing wave are nevertheless shown in Fig. 5, based on 50-term evaluations of the expansion (2.6). The nodal points of the seiches, corresponding to local maxima and minima of these three eigensolutions for the bulk horizontal displacement of the water mass, were found to be: $x = 0.51$ [0.51]; $x = 0.21$

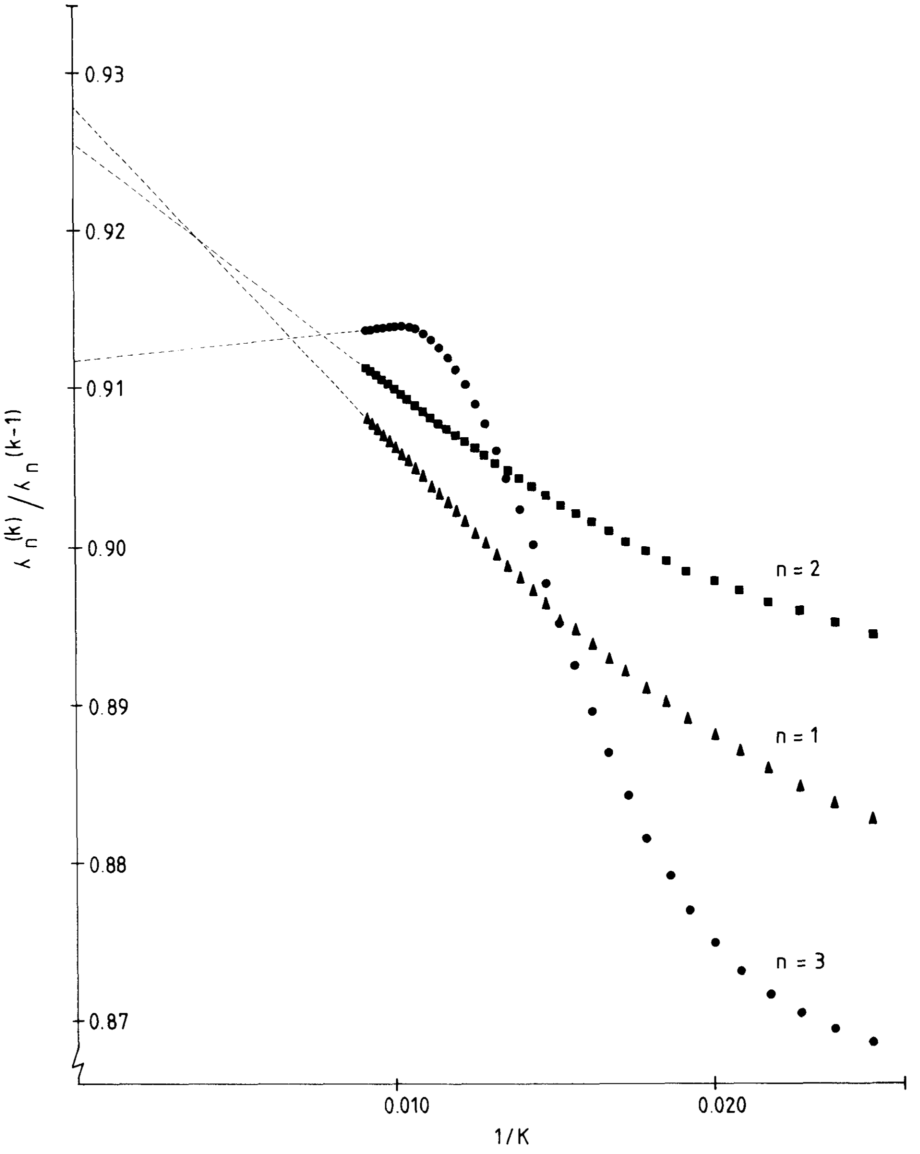

Fig. 4. Domb-Sykes plots of the eigenvalue expansion coefficients $\lambda_n^{(k)}$; $n = 1$, 2, 3 for the three gravest modes of the standing oscillation. For clarity, only the ratios based on the coefficients from $k = 40$ to $k = 110$ have been included in the graph.

and 0.73 [0.21 and 0.78]; $x = 0.15$, 0.50 and 0.87 [0.18, 0.58 and 0.95], where, for comparison, the values obtained from Bergsten's theoretical analysis have been included within brackets. It is seen that the agreement between the two sets of predictions decreases for the higher modes, but unfortunately, Bergsten's observational results (which were limited to the two gravest modes) are insufficiently precise to permit any comparison between the accuracy of the two computational schemes for determining the eigensolutions. For the third mode of the standing oscillation, no observational evidence concerning the location of the nodes was obtained during the original

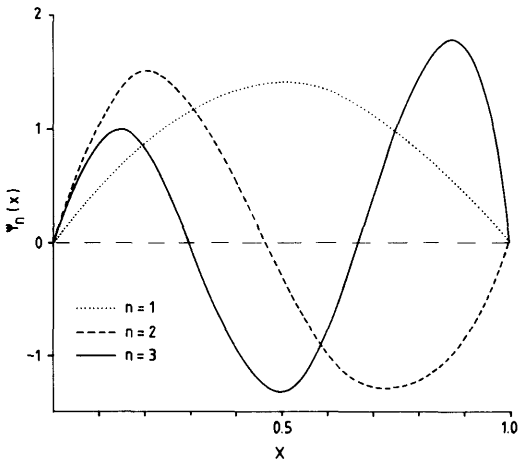

Fig. 5. The three normalized gravest-mode eigenfunctions of the problem, determined on the basis of 50-term perturbation expansions.

experiment. Bergsten, however, made the interesting observation that the amplitude of this seiche at the northerly end of the lake was around twice that registered at Jönköping, This asymmetry, which stands in marked contrast to the observed results for the first- and second-mode seiches, is fully borne out by the calculated third-mode eigensolution of Fig. 5, when this graph is interpreted in terms of surface elevations rather than bulk displacements of the water mass.

From Table 1, and in particular the agreement between the 50- and 100-term results, it appears evident that the convergence of the expansions does not pose any serious problem. (This was further verified by a considerable number of numerical experiments not reported here.) A more interesting feature of the table is that, independent of the order of the perturbation expansions, the theoretical predictions decrease in accuracy for the higher modes of the standing oscillation. The first- and second-mode results are of such quality that they may serve a useful purpose, but nevertheless, the intriguing question of what causes the successive degradation of the predictive value of the algorithm remains to be answered. Neglect of friction in the analysis could be invoked to at least partly account for the disagreement between observations and predictions; a well-known effect of damping in oscillatory systems is to decrease the eigenfrequencies. Recent results (Hukuda, 1986) furthermore indicate that this effect should be particularily pronounced for the higher seiche modes. The observed deviations are, however, of such a magnitude that it is highly questionable whether the entire discrepancy could be explained in terms of frictional damping (especially since the characteristic *e*-folding time of the standing waves was observed to be on the order of 35 h, yielding a friction coefficient of magnitude around 10^{-5} s^{-1}, cf. Defant (1961)). Similarly, neither the effects of lake stratification (LeBlond and Mysak, 1978) nor those of the earth's rotation (Defant, 1953), although both these factors act so as to decrease the eigenfrequencies, are sufficiently large to account for the observed deviations in the second- and third-mode results. A cause which appears more likely is that the lake topography may have been resolved with insufficient accuracy. This state of affairs should give rise to precisely the effects outlined above, since the higher seiche modes (with their shorter length-scales) can be expected to be progressively more sensitive to imperfections in the representation of the bathymetry. Against this background, it was also decided to undertake period calculations for normal curves of Lake Vättern based on different resolution than that employed by Bergsten.

Table 1. *Theoretically-determined periods of the three gravest modes of the standing oscillation for various truncation levels N of the perturbation expansions; also included are the results from the field observations; all values are given in min*

	$N = 10$	$N = 20$	$N = 50$	$N = 100$	Observed
T_1	178.66458	178.71809	178.72130	178.72134	179.5
T_2	93.26428	93.37675	93.38150	93.38159	97.0
T_3	66.03964	66.12052	66.12076	66.12123	80.5

4. Predictions using normal curves of lower resolution

When we attempted the construction of a more detailed normal curve $\sigma(v)$ than that provided by Bergsten (1926), it was recognized that no bathymetrical measurements had been undertaken in Lake Vättern since the beginning of last century when Sir Thomas Telford supervised a survey of the lake in conjunction with the planning of the Göta Canal. Any additional topographical cross-sections would hence have to be based on the same sparse observational material as that available to Bergsten. (These original soundings were furthermore made using hemp rope, which casts some doubt on their accuracy). In view of this state of affairs, it was decided instead to examine the effects of changing the topographical resolution by decreasing the number of points representing the normal curve. By only retaining every second data point, two reduced normal curves were ultimately obtained: a 15- and an 8-point version, both of which are shown in Fig. 6.

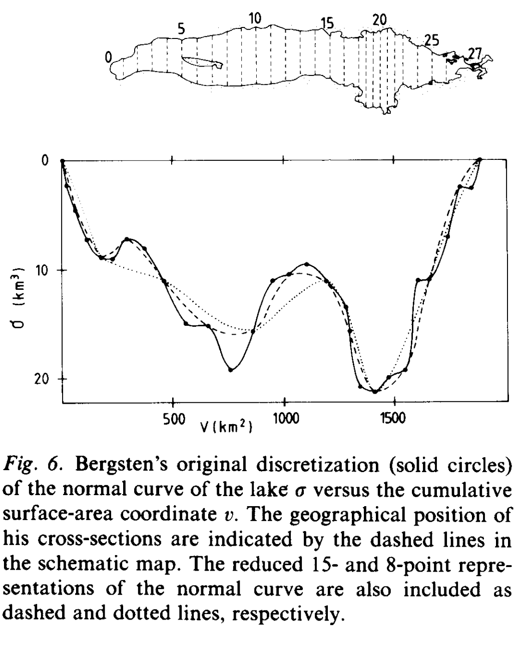

Fig. 6. Bergsten's original discretization (solid circles) of the normal curve of the lake σ versus the cumulative surface-area coordinate v. The geographical position of his cross-sections are indicated by the dashed lines in the schematic map. The reduced 15- and 8-point representations of the normal curve are also included as dashed and dotted lines, respectively.

Table 2. *Calculated periods for the three gravest standing-wave modes for 8-, 15- and 28-point representations of the normal curve; the perturbation expansions have been truncated after 30 terms; all values given in min*

	8 points	15 points	28 points
T_1	179.8323	179.1541	178.7209
T_2	95.8302	93.7456	93.3806
T_3	65.7347	69.7723	66.1200

The results from the calculations pertaining to these two "condensed" topographies are shown in Table 2, which also comprises the previously obtained periods from the 28-point analysis. (The computations were undertaken for 15- and 8-term Fourier-sine representations of the normal curve, respectively. A 30-term truncation level was used for the perturbation series, and the summations in the general recursive formulae for the expansion coefficients in these cases were also limited to 50 terms.) The overall impression gained from this table is that it appears unlikely that a more highly resolved normal curve would lead to any great improvements of the predictions for the higher modes. It is striking how stable the three gravest-mode periods are to the changes of the normal-curve representation, and how (in good agreement with qualitative considerations) the deleterious effects of too low a resolution first manifest themselves in the third-mode results, which show a slightly nonuniform behaviour.

These questions concerning the numerical effects induced by the various discretizations of the normal curve touch upon another matter of great importance, namely that of the accuracy of these representations. Since, as outlined above, the bathymetrical data for the lake is imprecise, it is not inconceivable that systematic errors may have entered the analysis due to an incorrectly prescribed normal curve. A sensitivity analysis, aimed at clarifying some aspects of this problem, will be outlined next.

5. Sensitivity analysis

A set of numerical experiments has been conducted in order to look at possible effects arising from incorrect estimates of the cross-sectional areas underlying Bergsten's normal curve. (The surface widths of these cross-sections were assumed to be unchanged, this in order to leave the cumulative horizontal coordinate of the mathematical problem unaffected.) The results

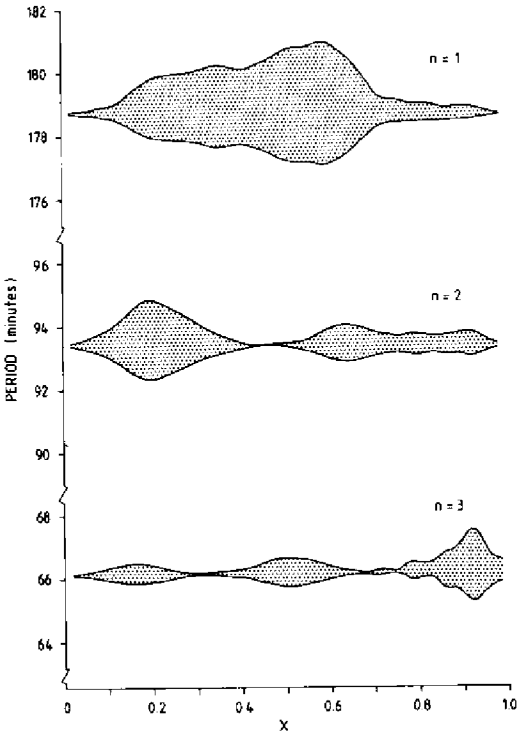

Fig. 7. Results of the sensitivity analysis for the three gravest modes of the seiche. The period envelopes, obtained by varying in turn each of the normal curve interior points $\pm 20\%$ from Bergsten's values, are shown. Note how well the regions of maximum sensitivity correspond to the nodal points of the standing waves.

obtained by varying in turn each of the interior normal curve points σ_k, $k = 1, 26$ over a range of $\pm 20\%$ from Bergsten's values are demonstrated in Fig. 7, where the resulting envelopes around the standard 50-term predictions from Table 1 are shown for the three gravest modes. (A decrease of the cross-sectional area corresponds to a lengthening of the seiche period, as may be recognized by interpreting the normal-curve changes as directly influencing the propagation velocity of the long wave.) From the graph, it is striking how well the regions of greatest sensitivity to topographical changes correspond to the locations of the nodal points (where the largest horizontal velocities are encountered and consequently where changes of the cross-sectional area can be expected to exert particularly effective controlling influence.) The spatial separation of these maxima is, as will be shown, also highly interesting when attempts are made to impose corrections on the computational results.

The gravest-mode seiche is, in a relative sense, least affected by perturbations of the normal curve, and furthermore is seen to be markedly insensitive to topographic changes over the most northerly part of the lake. The second mode of the standing wave shows a pronounced sensitivity maximum at around $x = 0.2$. This region not only includes the most southerly nodal point of the seiche, but also coincides with the location of Visingsö Island (cf. Fig. 1). It is reasonable to assume that the existence of this island tends to decrease the effective cross-section available for flow below the directly calculated area value employed by Bergsten for his predictions. Against this background, a numerical experiment was undertaken where the normal-curve points 5, 6 and 7 were simultaneously reduced by 10, 20 and 10%, respectively, in which case the 50-term results for the three gravest-mode periods became $T_1 = 180.098$, $T_2 = 95.595$, and $T_3 = 66.703$ min. By comparing with the original predictions of Table 1, it is recognized how selectively this topographic change has limited itself to primarily affecting the second mode of the standing oscillation, the first and third modes remaining almost unchanged. It thus appears as though the discrepancy between observations and predictions of the second-mode period may, to a large extent, be explained in terms of the constricting effects of Visingsö Island.

When attention is directed towards the third mode, a more complex picture emerges. By retaining the correction for cross-sections 5, 6 and 7 introduced above and simultaneously reducing the normal curve by 20% for sections 23, 24 and 25, (where the third-mode sensitivity has an overall maximum associated with the most northerly node), the following periods were obtained: $T_1 = 180.634$, $T_2 = 96.580$ and $T_3 = 69.477$ min. The third-mode period discrepancy of Table 1 was, however, around 15 min, and it cannot be accounted for solely on the basis of this effect, even if the magnitude of the nodal region topographic correction is considerably increased. Nevertheless, these results serve as an indication of a mechanism which could possibly come into play; when the cross-sectional areas 25 and 26 were reduced by 50 and 67%, respectively, the third-mode discrepancy was drastically reduced, whereas the first- and second-mode periods remained almost unchanged: $T_1 = 180.791$, $T_2 = 97.616$ and $T_3 = 74.705$ min. These numerical calculations of the three gravest-mode seiche periods conform in an overall sense much more closely to the spectral peak locations of Fig. 3 than any of the previously computed results, and hence it appears reasonable to ascribe the difference between the third-mode observations and the original prediction to insufficient knowledge of the detailed lake topography in the vicinity of Askersund.

No effects of comparable size were recorded when cross-sections 1 and 2 immediately adjacent to Jönköping were manipulated in the same manner. This "asymmetrical" response indicates that what has been observed from the numerical experiments is not merely a boundary effect, but rather represents a fundamental dependence of the third-mode seiche upon the topographical conditions in the extreme north of the lake. To judge from the data presented above, it moreover appears far from unlikely that this sensitivity may be of such a magnitude so as to possibly account for the discrepancy between the observed and calculated periods of the third-mode standing wave. From a predictive standpoint, this skewed topographical dependence is unfortunate, since the lake bathymetry, as evident from Fig. 1, is most complex at the northern end of the lake. This does not facilitate good estimates of the cross-sectional areas, and hence there may be some reason to assume that errors of this type have crept into the original normal curve data. For Bergsten's calculations, these inaccuracies were of no consequence due to the many degrees of freedom available when fitting his polynomial approximations to the normal curve, but for the present computational method, which relies on a much more exhaustive use of the available data, far from negligible errors have been introduced into the results.

This discussion of the sensitivity problem may be concluded by noting that similar effects were observed for perturbations of the lake surface area, i.e., the cumulative horizontal coordinate used in the calculations. Retaining the previously introduced corrections for cross-sections 5, 6 and 7, a 50% increase of the surface areas between sections 25, 26 and 27 yielded the following 50-term results: $T_1 = 184.835$, $T_2 = 99.362$ and $T_3 = 74.943$ min. Hence, the third-mode prediction was affected in the most selective fashion also for this type of topographic modification applied at the northern end of the lake. No systematic investigation of this dependence was undertaken, but to judge from the quoted result, it most likely also plays a rôle in determination of the overall results of the numerical computations.

6. Discussion and conclusions

From the analysis of Section 5, it appears as though the 4-min discrepancy between the observations and predictions of the second-mode standing oscillation can be ascribed in a rather straightforward manner to the constricting effects of Visingsö Island, located at the most southerly node of the seiche. The mechanism underlying the 15-min third-mode discrepancy is more subtle, not least since it could be demonstrated that topographical corrections of reasonable magnitude applied in the most sensitive nodal-point region of the standing wave did not suffice to account for the entire difference. Numerical experiments indicated that the lack of agreement may instead by caused by overestimates of the lake cross-sectional area (and/or underestimates of the surface area) at the extreme north of the basin. This conclusion is further borne out by the observation that when the computational algorithm derived here was applied to the polynomial representation of the normal curve due to Bergsten, perfect agreement with his predictions (and consequently also with the observations) was obtained. Except for the northernmost cross-sections of the basin, the deviations between this polynomial approximation and the original 27 points of the normal curve are smaller than those shown by the reduced-point representations of Fig. 6, for which the computed standing-wave periods are given in Table 2. Although the higher-mode results are slightly off the mark, these sets of predictions are internally remarkably uniform, and hence it has been concluded that Bergsten's very accurate theoretical calculations cannot be ascribed to his polynomial representation of the normal-curve interior points. The explanation appears instead to be that (as is evident from a careful inspection of Bergsten's original figures) the polynomials have been chosen so as to obtain a sharply wedged northern termination of the normal curve, i.e., precisely the effect achieved by the cross-sectional and surface-area corrections applied in Section 5 of this study. That standing waves can be extremely sensitive to topographic features of this type has been demonstrated in another context by Lundberg (1989), and in the present case, this strong dependence upon the end-point geometry of the basin is further corroborated by the Domb-Sykes plots of Fig. 4. From this, it is recognized that, contrary to intuitive expectations, the radii of convergence of the eigenvalue expansions increase for the higher modes of the standing oscillation. The explanation most likely can be found in the geometrical properties of the eigenfunctions as demonstrated in Fig. 5. When interpreted in terms of surface elevations rather than bulk horizontal displacements of the water mass, this graph shows that at the northern end of the lake, the higher-mode free surfaces "intersect" the normal curve at progressively larger angles (i.e., in a less singular fashion), a state of affairs which is reflected in the convergence properties of the perturbation expansions.

The overall impression gained from the results of this study is that the disagreements between observations and model predictions as summarized in Table 1 may be accounted for in terms of unsatisfactory knowledge of the lake bathymetry (including the difficulty of quantifying the constricting effects of Visingsö Island). Other explanations are conceivable; a breakdown of the validity of the canal approximation does not, however, appear very likely, since the lake is both straight and narrow, viz., an almost ideal shape. The small width of the lake furthermore tends to preclude the occurrence of rotational effects, and the frictional damping is too weak to explain the observed discrepancies. It has thus been concluded that the perturbation scheme for determining seiche periods derived in this study is a useful tool, and that the shortcomings of the present theoretical investigation could most likely be remedied, were better topographical data available.

An important question, namely whether the "Chrystal methodology" still can be regarded as an adequate framework for the description of barotropic seiches in elongated lakes, can most likely be answered in the affirmative. Recent results (Hutter and Raggio, 1982; Lemmin and Mortimer, 1986) strongly underline that it is a highly useful technique, provided that the basin under study is sufficiently straight and narrow, conditions which Lake Vättern evidently fulfill. Note, however, that possible shortcomings of the model in these respects can only be investigated using numerical techniques (Platzman, 1972), a task well beyond the scope of this study.

Finally it may be remarked that one interesting aspect of the standing-wave problem, which has been neglected in the present investigation, concerns the forcing mechanism giving rise to the seiche motion. The initial set-up of the water mass is meteorological in origin, but the question remains to be answered whether wind stress or differential barometric pressures along the lake is most efficient in this respect. Routine weather observations are available from the air-fields in Karlsborg and Jönköping, and ongoing work should presumably be able to resolve this question within the near future.

7. Acknowledgements

This work was supported by the Swedish Natural Science Research Council under contract NFR-G-4768. The authors are grateful to Anders Björk of Jönköping for overseeing the water level gauge during the period of operation, and, furthermore, thank two anonymous reviewers for valuable comments and suggestions.

REFERENCES

Bergsten, F. 1926. The seiches of Lake Vetter. *Geogr. Ann. 8*, 1–73.

Båth, M. 1974. *Spectral analysis in geophysics*. Amsterdam, Elsevier, 563 pp.

Chrystal, G. 1904. Some results in the mathematical theory of seiches. *Proc. R. Soc. Edinb. 25*, 328–337.

Chrystal, G. 1905. Some further results in the mathematical theory of seiches. *Proc. R. Soc. Edinb. 25*, 637–647.

Defant, F. 1953. Theory for the standing waves of Lake Michigan are how they are influenced by the Coriolis force. *Arch. Met. Geoph. Biokl. Ser. A 6*, 218–241.

Defant, F. 1961. *Physical oceanography, vol. II.* Oxford, Pergamon Press, 598 pp.

Domb, C. and Sykes, M. F. 1957. On the susceptibility of a ferro-magnetic above the Curie point. *Proc. R. Soc. London Ser. A 240*, 214–228.

Ertel, H. 1933. A new method for calculating standing-wave motion in lakes of irregular shape. *S.B. Preuss. Akad. Wiss., Phys.- Math. Kl. 24*, 746–750.

Hukuda, H. 1986. On the damping of gravity oscillations in closed basins. *Dyn. Atmos. Oceans 10*, 97–109.

Hutter, K. and Raggio, G. 1982. A Chrystal-model describing gravitational barotropic motion in elongated lakes. *Arch. Met. Geoph. Biokl. Ser. A 31*, 361–378.

LeBlond, P. H. and Mysak, L. A. 1978. *Waves in the ocean.* Amsterdam, Elsevier, 602 pp.

Lemmin, U. and Mortimer, C. H. 1986. Tests of an extension to internal seiches of Defant's procedure for determination of surface seiche characteristics in real lakes. *Limnol. Oceanogr. 31*, 1207–1231.

Lundberg, P. A. 1989. Some further results on slightly nonhydrostatic standing waves. *Acta Hydrophys. 33*, 125–145.

Lundberg, P. A. 1990. Determination of seiche periods using the Rayleigh-Schrödinger technique. *Z. Angew. Math. u. Mech.*, in press.

Platzman, G. W. 1972. Two-dimensional free oscillations in natural basins. *J. Phys. Oceanogr. 2*, 117–138.

Raggio, G. and Hutter, K. 1982. An extended channel model for the prediction of motion in elongated homogeneous lakes, Parts 1–3. *J. Fluid Mech. 121*, 231–299.

Shanks, D. 1955. Non-linear transformations of divergent and slowly convergent sequences. *J. Math. & Phys. 34*, 1–42.